AIAA 2000-1044

Parametric Model of an Aerospike Rocket Engine

J. J. Korte
NASA Langley Research Center
Hampton, Virginia

38th Aerospace Sciences Meeting & Exhibit
10-13 January 2000 / Reno, NV

PARAMETRIC MODEL OF AN AEROSPIKE ROCKET ENGINE

J. J. Korte*

NASA Langley Research Center, Hampton, Virginia 23681

Abstract

A suite of computer codes was assembled to simulate the performance of an aerospike engine and to generate the engine input for the Program to Optimize Simulated Trajectories. First an engine simulator module was developed that predicts the aerospike engine performance for a given mixture ratio, power level, thrust vectoring level, and altitude. This module was then used to rapidly generate the aerospike engine performance tables for axial thrust, normal thrust, pitching moment, and specific thrust. Parametric engine geometry was defined for use with the engine simulator module. The parametric model was also integrated into the iSIGHT[†] multidisciplinary framework so that alternate designs could be determined. The computer codes were used to support in-house conceptual studies of reusable launch vehicle designs.

Nomenclature

A	cross-sectional area
a	constant in Eq. (7)
AR	area ratio
b	constant in Eq. (7)
E	energy
F	force
h	enthalpy
M	Mach number
$\dot{m}$	mass flow
MR	mixture ratio
p	pressure
PL	power level
T	temperature
x	axial coordinate
y	normal coordinate
γ	ratio of specific heats
ε	constant in Eq(6)
η	efficiency
θ	thruster tilt angle
ρ	density

subscripts

b	base
c	combustor
cowl	cowl
f	fuel (H2)
g	gas generator
o	oxidizer (O2)
t	turbine
T	total
thr	thruster
w	wall

x	axial direction
y	normal direction

Introduction

Launch vehicle performance is evaluated by computing the optimum vehicle trajectory. One part of the essential data for an accurate trajectory simulation is the engine performance (Fig. 1).
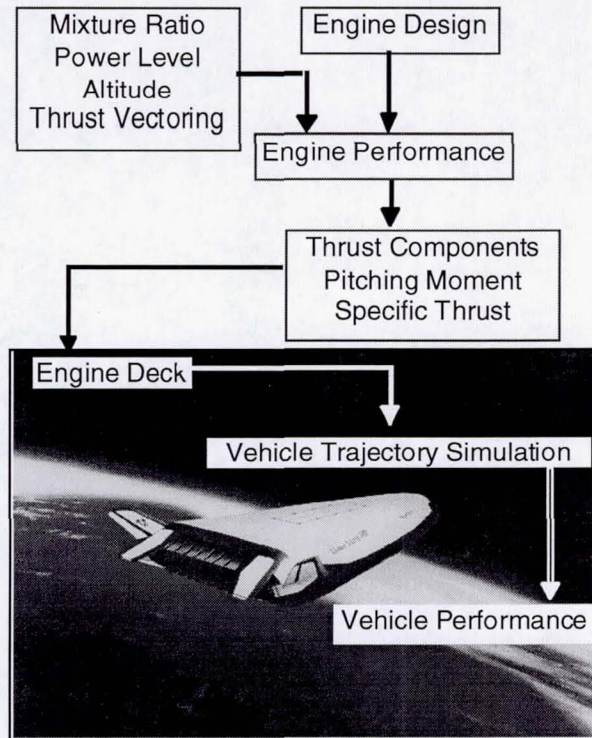

Fig. 1 Engine data needed for vehicle trajectory simulation.

Lockheed Martin's[†] reusable launch vehicle concept, the VentureStar™,[1,2] proposes to use an aerospike rocket engine. The aerospike engine performance is significantly more complicated than a traditional bell nozzle rocket engine[3] since the proposed aerospike engine has variable mixture ratio and power levels, is capable of thrust vectoring, and has a complex flow structure that affects the performance of the engine as the vehicle ascends through the atmosphere.

The aerospike rocket engine consists of a gas generator, turbopumps, combustor, rocket thruster, cowl, aerospike nozzle, and plug base region (Fig. 2).

The gas generator and turbopumps are packaged between the upper and lower aerospike nozzle surfaces (Fig. 3).
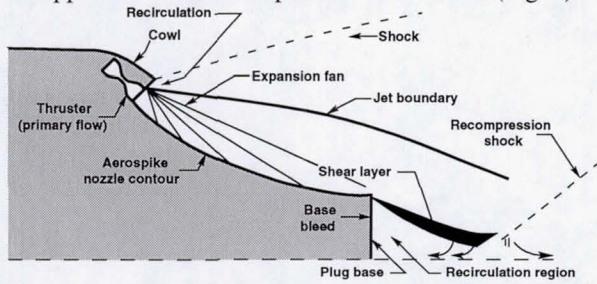

Fig. 2 Aerospike components and flow-field characteristics shown for the upper half of the aerospike engine.

The aerospike nozzle is a truncated spike (or plug nozzle) that adjusts to the ambient pressure and potentially integrates well with launch vehicles. The flow-field structure changes dramatically from low altitude to high altitude on the spike surface (Fig. 3) and in the base region.[4-6] Figure 3 shows the pressure contours for the hot exhaust gas expanding along the aerospike nozzle surface for different altitude conditions. The top contour is for an altitude slightly less than the nozzle design condition (at the design condition, the upper boundary would be parallel to the vehicle centerline). The bottom contour is for an altitude near sea level. Near sea level, the atmospheric pressure is close to the exhaust gas pressure such that it does not expand significantly, and therefore follows the nozzle contour until the flow has turned enough to create a shock near the end of the nozzle.
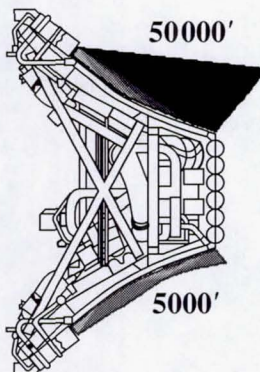

Fig. 3 Computed inviscid pressure contours for the exhaust gasses at different altitude conditions. The Upper half of figure shows a pressure contour near the design point and lower half of the figure, near sea level.

The base region creates an aerodynamic spike[7] at high altitudes (giving the aerospike its name), thus maintaining the base pressure and the contribution of the base region to the aerospike thrust. In the early 1960's, aerospike and plug nozzles were the focus of development projects in the United States,[7] Italy,[8] Germany,[5] and Soviet Union.[9] More recently, they have been proposed as the propulsion system for the reusable launch vehicle (RLV) program for NASA[2] and have been studied in the Advanced Rocket Propulsion Technologies[10] and Future European Space Transportation Investigations

Programme[11] for European Space Agency. They are also being studied in Japan.[12,13]

In support of the NASA RLV program, a group was formed at NASA Langley Research Center to help mature the VentureStar vehicle concept with Lockheed Martin Skunkworks and their partners.[14] Conceptual vehicle analysis typically uses simplified relationships for propulsion data accurate for bell nozzle rocket engines but not applicable for predicting thrust vectoring capability of an aerospike rocket engine. This paper addresses the problem of generating an aerospike engine database for use in the POST (Program to Optimize Simulated Trajectories).[15]

Method

An aerospike rocket engine of the type required for powering a VentureStar class vehicle has not been tested or designed in detail. Typical engine data for an RLV class vehicle is given in Table 1. Part of the conceptual vehicle design process is determining both the required engine thrust and the number of engines needed. During the conceptual design of a vehicle, a number of different engine designs were evaluated. For each new aerospike engine, the conceptual design team obtained limited performance estimates at five critical trajectory points from Rocketdyne, the propulsion contractor. Initially, these estimates were limited due to the concentration of resources on the development of the X-33 RLV. These initial estimates were based on engine gas generator cycle analysis and a calibrated approximation of an aerospike nozzle's performance (from extrapolation of experimental data). The initial, limited propulsion data did not include the nozzle forces and moments necessary for controlling vehicle pitch angle along a trajectory. In addition to nozzle forces and moments for controlling pitch, more data points were needed to accurately optimize the vehicle trajectory. For these reasons, an alternate but compatible method was developed for predicting aerospike engine performance.

Table 1: Aerospike Engine Description Data

RS-2200 Engine	At Sea Level	In Vacuum
Thrust, lbf	520,000	564,000
Specific Impulse, sec	342	456
Propellants	Oxygen,	Hydrogen
Mixture Ratio (O/H)	6.0	5.5
Chamber Pressure, psia	2,250	1,950
Cycle	Gas	Generator
Area Ratio	193	
Throttling, Percent Thrust	20~100	20~84
Dimensions, inches Forward End Aft End Forward to Aft	294 wide x 120 wide x 175	96 long 96 long

<www.boeing.com/space/rdyne/x33/rlv/rs2200/eng_data .htm> (Nov. 15, 1999)

A suite of computer codes was assembled to simulate the performance of an aerospike engine and to generate the engine input for POST. An engine simulator module

was developed; the module was able to predict the aerospike engine's performance for a given mixture ratio, power level, and altitude. This module was then used to generate the aerospike engine performance for axial thrust, normal thrust, pitching moment, and specific thrust.

The aerospike engine module simulated or modeled the gas generator, combustor, aerospike nozzle flow field, and nozzle base region. An algebraic relationship was derived for the gas generator to estimate the amount of hydrogen and oxygen necessary for operation.[16] The algebraic equations were calibrated with engine cycle results. The engine cycle results used were similar to the data presented by Erikson.[17] Subsequently, the combustor mixture ratio was determined for a given total engine mixture ratio. The combustor was simulated with an equilibrium chemical reaction. The thruster exit condition was obtained by calculating a one-dimensional expansion process in chemical equilibrium.[18] The thruster exit condition was used as an inflow boundary condition for a space marching computational fluid dynamics code[19] that provided a two-dimensional solution to the Euler equations. The base flow thrust contribution was estimated as a function of the total engine area ratio. One thrust cell and nozzle were simulated at a time. The axial and normal thrust, specific fuel consumption, and pitching moment were determined for each flow condition. Realistic performance was obtained by applying engine loss factors for combustion, flow divergence, and boundary layer losses.[20]

The engine module was written so that the geometry and flow conditions of the aerospike engine could be used as design variables in an optimization problem. Likewise, the engine performance parameters are available for use as potential objective functions. The aerospike nozzle contour can be described either with a set of coordinates or by control points for a cubic spline. The engine module was coupled with the iSIGHT framework[21] so that multidisciplinary design issues could be investigated. The resulting codes can be used either to evaluate an existing design or to determine alternate ones.

Aerospike Engine Parametric Model

The parametric model of the aerospike rocket engine is divided into the simulation of four major areas: (1) the gas generator cycle, (2) the combustor, (3) the thruster, and (4) the aerospike nozzle. These capabilities were added to the existing computer codes developed for multidisciplinary analysis of an aerospike nozzle, reported in Korte et al.[19]

Gas Generator Cycle

According to Erikson,[17] the most efficient power cycle for the aerospike rocket engine is the gas generator. A portion of the fuel and oxygen is burned in a gas generator to power both the fuel and oxygen turbines (Fig. 4). The energy generated by the turbines is used to power the pumping of the hydrogen and oxygen propellants from the tanks into the combustor. Very

detailed computer models (cycle analysis codes) of this process, which include detailed models of the plumbing, cooling system, turbines, and pumps, have been developed by industry. For this effort, we are only concerned with the amount of the total flow of propellants that the gas generator uses for a given operating condition. We were given five points and needed to extrapolate the data across the engine's operational envelope. The mixture ratio of the gas generator (MR_g) and of the engine (MR_T) are given, along with some of the gas generator parameters. The mixture ratio of the combustor (MR_c) has to be determined for computing the combustor state.
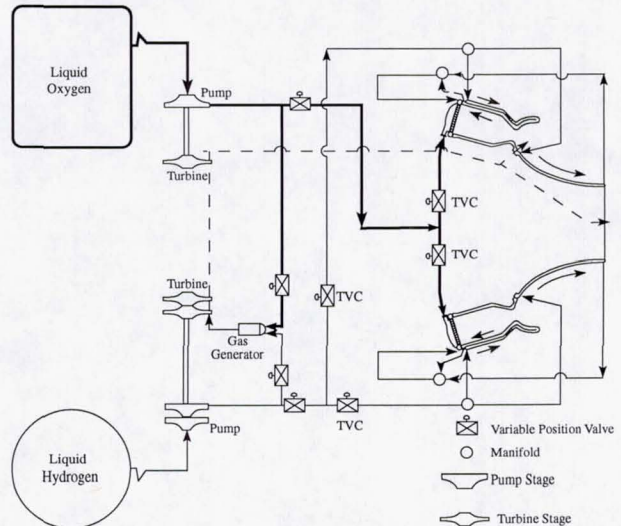

Fig. 4 Gas generator and turbopump system.

Erikson analyzed a typical gas generator system that used two turbines in series for turning the pumps (Fig. 4). The energy equations for the turbine and the pump are defined by using the relationships from Schmucker.[16]

$$E_t = \dot{m}_g \Delta h_t \eta_t \tag{1}$$

$$E_p = \frac{\dot{m}p}{\eta_p \rho} \tag{2}$$

In Eq. (2), the pressure is referring to pump outlet, and it is valid only if the pump inlet pressure is small and can be neglected. The pump outlet pressure is dependent on the engine power level setting and the delivery system pressure drop:

$$P_o = p_c + \Delta p_o, \quad p_f = p_c + \Delta p_f \tag{3}$$

The mixture ratios are related to the mass flows by

$$MR_T = \frac{(\dot{m}_g + \dot{m}_c)_o}{(\dot{m}_g + \dot{m}_c)_f}, \quad MR_c = \left(\frac{\dot{m}_o}{\dot{m}_f}\right)_c, \quad MR_g = \left(\frac{\dot{m}_o}{\dot{m}_f}\right)_g \tag{4}$$

and the mass flows are related by

$$\dot{m}_T = \dot{m}_g + \dot{m}_c = (\dot{m}_o + \dot{m}_f)_T = [(MR_T + 1)\dot{m}_f]_T \tag{5}$$

Equating the energy used by the pump and the turbine, one finds

$$\frac{\dot{m}_g}{\dot{m}_T} = \varepsilon \times f(MR_T, PL) \tag{6}$$

where ε is a constant coefficient calculated so that the equation result agrees with the engine cycle data. With the

American Institute of Aeronautics and Astronautics

cycle performance data given by Erikson, ε was computed to be 0.94, showing that the model yields a reasonable approximation of the cycle analysis. The combustor mixture ratio can then be calculated by

$$MR_c = \frac{\left(MR_T(1+b)-a\right)}{\left(1+a-b\times MR_T\right)} \quad (7)$$

where

$$a = \frac{\dot{m}_g MR_g}{\dot{m}_c\left(MR_g+1\right)}, \quad b = \frac{\dot{m}_g}{\dot{m}_c\left(MR_g+1\right)},$$

$$\text{and} \quad \frac{\dot{m}_g}{\dot{m}_c} = \frac{\dot{m}_g/\dot{m}_T}{1-\left(\dot{m}_g/\dot{m}_T\right)} \quad (8)$$

The relationship for p, ρ, Δh_r, η_r and η_p as a function of power level and mixture ratio was curve fitted from the five points obtained from the power cycle analysis. Solving the above equations gave reasonable agreement for both the combustor mixture ratio and the amount of mass flow needed to operate the gas generator.

Combustor and Thruster

The combustion chamber of an aerospike is similar to other rocket engines except that each power pack (gas generator and turbopump system) supplies a row of combustion chambers on both the top and bottom of the engine. Each combustion chamber is connected to a thruster nozzle. The thruster nozzle is a three-dimensional design to enable efficient volumetric packaging and minimum turning losses when the exhaust flow intersects the aerospike nozzle.[22] The thruster nozzle is tilted at an angle toward the vehicle centerline. Once the combustor mixture ratio and total pressure is known, the total enthalpy of the mixture can be computed by assuming an equilibrium reaction of hydrogen and oxygen. The exit condition for the thruster is computed by expanding the flow to the desired thruster area ratio, assuming chemical equilibrium and one-dimensional characteristics. The contribution of the thruster to the axial thrust and normal thrust can then be calculated by using one-dimensional flow equations

$$F_{x-thr} = pA\left(1+\gamma M^2\right)\cos\theta \quad (9)$$

$$F_{y-thr} = pA\left(1+\gamma M^2\right)\sin\theta \quad (10)$$

where p, A, γ, M, and θ are static pressure, cross-sectional area, ratio of specific heats, Mach number, and thruster tilt angle (with respect to the horizontal axis), respectively.

Aerospike Nozzle

The aerospike nozzle contour starts at the exit of the thruster nozzle and extends to the end of the engine. The nozzle contour is usually determined by designing a spike nozzle and then truncating it. Traditionally the contour of the aerospike nozzle has been designed by using both simple methods[23,24] and more elaborate methods based on calculus of variations.[25-27] These design approaches are adequate for determining an aerodynamic contour that satisfies a design for maximum thrust at one design condition (high altitude condition). The aerospike contour design is usually modified as the design of the engine progresses. For example, the length of the nozzle may be varied to improve the thrust-to-weight ratio of the engine. In addition to structural weight effects, the thermal cooling system, propulsion-vehicle integration, thruster contour, and the fuel-oxidizer delivery system are a few of the issues that are significant in the aerospike nozzle contour design.

The pressure distribution on the nozzle contour is calculated by using a space marching parabolized Navier-Stokes code.[28] The computational domain begins at the end of the thruster nozzle and ends at the nozzle exit. The domain is bounded by the nozzle wall on the bottom and the flow expansion on the top. The combustion product was assumed to be water in vibrational equilibrium. The flow that exits the thruster onto the nozzle is assumed to be spatially uniform and chemically frozen. The computed flow field is equivalent to an Euler flow-field solution because the boundary condition at the nozzle wall was a slip-wall condition. The computational grid uses 60 points in the normal direction and approximately 2000 streamwise stations. The computed pressure distribution was integrated to obtain the aerospike nozzle's contribution to axial and normal forces and pitching moment.

Base Region and Gas Generator Exhaust

The base region is where a complex interaction occurs among the nozzle and vehicle aerodynamics, the atmosphere, and the exhaust of the gas generator. Depending on the atmospheric pressure, the nozzle wake may be either open or closed. At low altitudes, the wake is open allowing the base pressure to be near the freestream conditions. At higher altitudes the nozzle wake closes. The base pressure then becomes independent of altitude as the vehicle continues to climb. The base pressure for the closed wake condition can be increased (up to a limit) by introducing additional mass flow. The exhaust flow from the gas generator supplies the gas for the base bleed. Predicting the base region performance by either experimental or numerical means is extremely difficult. For conceptual design, the many details needed for numerical simulation are not well known. Most predictions for conceptual design rely on an historical database of experiments and detailed numerical computations. Theoretical bounds for the thrust contribution can be established by treating the truncated nozzle and the exhaust flow separately.

One way to estimate the maximum performance of the base is to assume that the aerospike expansion process is identical to that of a full-length nozzle. The ideal specific impulse (ISP) for the full area ratio can be calculated and subtracted from the ISP calculated for a truncated nozzle. The ISP calculated for the truncated nozzle is lower than for a perfectly expanded nozzle—a nozzle of a reduced area ratio based on the base height—because the flow has not been completely turned to be parallel with the vehicle centerline at the end of the truncated nozzle. For example, the maximum ISP contribution of the base for

the engine specification given in Table 1 is approximately 7 seconds, due to area ratio effect and an additional 57 seconds for nonparallel flow effects. The base region has the theoretical potential to provide an additional 14 seconds of ISP when the wake is closed.

In practice, the base region has to be pressurized with a gaseous bleed to improve recovery. The questions that need to be answered are what fraction of the theoretical contribution is obtained and how much of the gas generator exhaust is needed to obtain it? The answers to these questions are important because the massflow from the gas generator has the capability to augment thrust. Erikson's calculation demonstrates that the gas generator uses about 3.4% of the total mass flow.[17] If the gas generator does not produce any additional thrust, this equates to a theoretical maximum loss of approximately 16 seconds of ISP (for an area ratio of 193). If we assume that the gas generator massflow could provide thrust with a sonic nozzle (about 300 sec ISP), then the penalty would only be approximately 6.5 seconds of ISP. However, expanding the gas generator massflow is not always possible because some or all of it may be diverted to help cool hot structures.

In this study, we were provided engine ISP performance estimates at both vacuum and sea level conditions, along with everything necessary to estimate the performance of the engine up to the end of the aerospike. The fraction of thrust contribution from the base and the gas generator exhaust was adjusted to ensure the performance estimates matched at these points. This adjustment was based on determining the fraction of the theoretical base pressurization and gas generator thrust needed to obtain the expected performance.
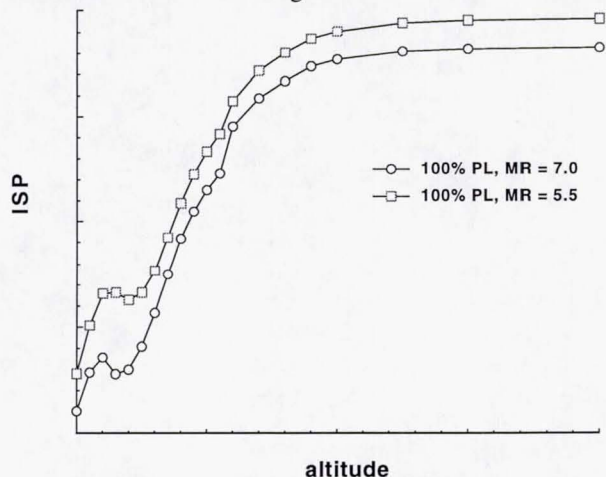
Loss Factors

The mass flow, thrust, and moments for the engine were computed assuming ideal conditions. The computed results were adjusted with efficiency factors for combustion effects, flow divergence, and boundary layer drag. These factors were the typical efficiencies used to compare rocket engine predicted performance with experimental data.[16] These efficiencies were included in the engine data at the five operating points. However, because we have unbalanced normal forces and moments acting on the aerospike engine when operating in thrust vectoring mode, the boundary layer drag loss factors were treated specially.

A boundary layer solution was computed for both vacuum and sea level conditions. A representative thruster geometry was modeled with an aerospike nozzle contour. The axial and normal drag force and pitching moment were calculated for the different conditions. The axial drag computed from the boundary layer analysis agrees favorably with the drag computed from the supplied boundary layer efficiencies. Factors were defined and were multiplied by the computed axial drag to obtain the normal drag force and pitching drag moment. These factors were then used for estimating the boundary
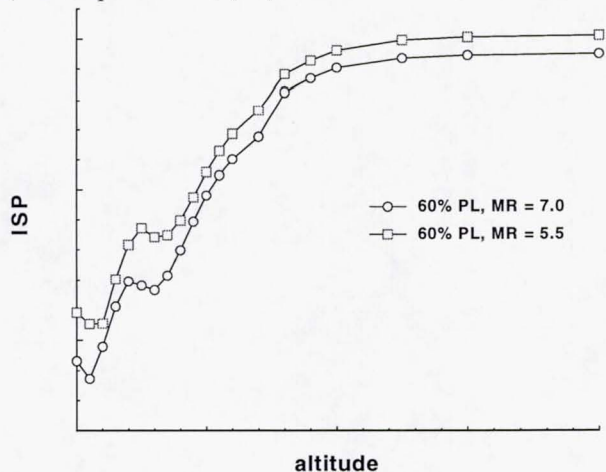
layer drag at each point instead of running a separate boundary layer calculation.

Performance Estimates

The calculation of engine performance with the above defined strategy at a given power level, mixture ratio, and altitude takes approximately 15 seconds on a SUN Ultra™ 2 computer. To define the performance for thrust vectoring requires two analyses. Even though the total mass flow is the same for a thrust vector control (TVC) case, the combustor pressures are different in the upper and the lower halves of the engine. A computer code was written to generate a POST engine deck by repeatedly executing the aerospike parametric model as a function of mixture ratio, power level, thrust vectoring, and altitude until all engine operating points had been simulated. The mapping of the design space into a POST deck usually took about 3 hours (approximately 1200 cases). Typical ISP results are shown in Fig. 5.
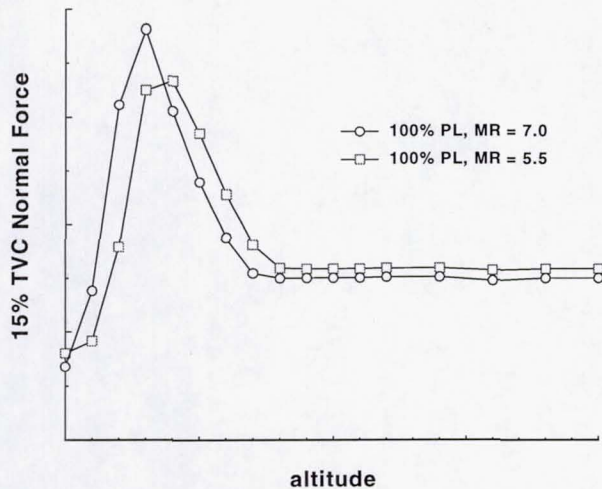

a) 100% power level (PL).

b) 60% power level.

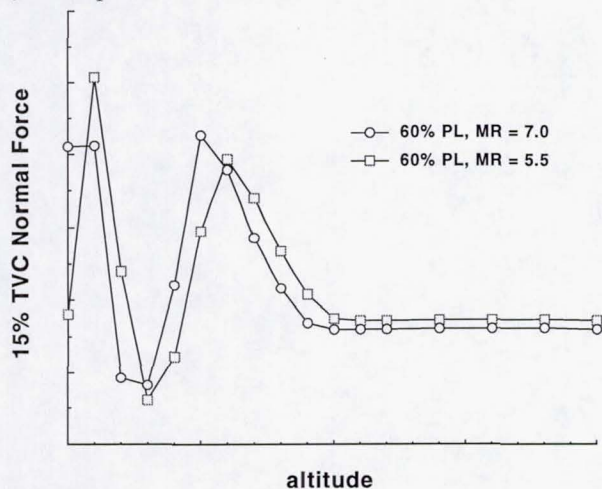Fig. 5 ISP trend with altitude for two different mixture ratios.

A characteristic of the aerospike at low altitudes is that a shock will hit the nozzle wall. This phenomenon can clearly be seen (in Fig. 5a for one shock reflection and in Fig. 5b for two shock reflections) by the local decrease in

American Institute of Aeronautics and Astronautics

ISP as the altitude increases. The second characteristic of the aerospike is the small altitude range where the base region changes from an open wake to a closed wake. This effect can be observed by the change in the local slope of the ISP near the vacuum condition.

The TVC forces are obtained by shifting the power levels of the upper and lower combustors while maintaining the same average engine power level. To simulate the maximum positive TVC forces and moments, the top aerospike stagnation pressure is increased by 15% and the lower aerospike stagnation pressure is lower by 15% while using the same overall mixture ratio. The TVC forces and moments are summed at the centerline of the vehicle at the axial location of the engine cowl. Two power levels are shown in Fig. 6. The aerospike nozzle characteristics are that the TVC forces are very nonlinear for the lower altitudes and can be significantly higher than the TVC forces obtained in vacuum.

a) 100% power level.

b) 60% power level.

Fig. 6 Computed normal force for 15% thrust vector control versus altitude for two different mixture ratios.

A similar trend is obtained with the pitching moment (Fig. 7). The vehicle center of gravity (cg) is farthest

from the engine at the beginning of the flight. As the fuel is consumed, the cg moves toward the engine, reducing the moment arm acting with the TVC force. The highly nonlinear behavior of the normal forces and pitching moments will make controlling the pitch angle of the vehicle more difficult because the amount of pitch correction obtained with a fixed amount of TVC can change rapidly with altitude. Both the normal force and the pitching moment are significant in controlling the vehicle pitch angle.
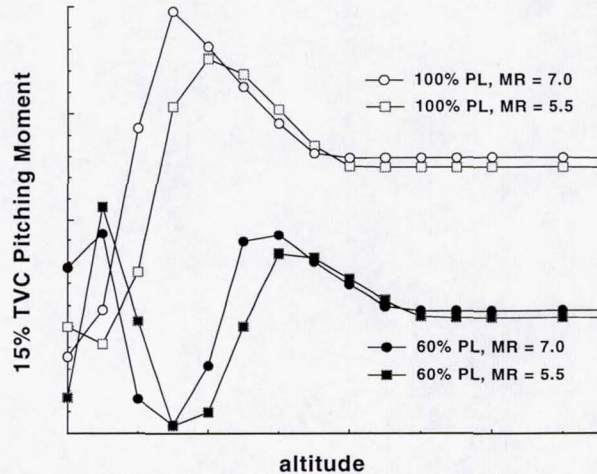

Fig. 7 Predicted pitching moment for 15% thrust vector control versus altitude for two different mixture ratios and power levels.

The described methodology has been used to define a number of aerospike engines designed for use in our conceptual vehicle studies.

Sample Engine Design With iSIGHT Framework

The engine codes have also been incorporated into a multidisciplinary framework code, iSIGHT, to allow for alternate designs based on more integrated design objectives. Examples of different problems solved with the iSIGHT framework are given by Padula et al.[29] A sample design problem is defined for the aerospike engine specifications given in Table 1. The aerospike engines are designed to fill a base region and sized to generate the required sea level thrust. The sample engine from Table 1, is required to deliver 520,000 lbf at sea level and to fill a vehicle base that is 294 inches wide by 96 inches long. The width refers to the width of the engine in the vertical position (vertical launch), and length is the distance across the engine in the vehicle spanwise direction. The sample design problem is to determine the engine thruster angle, thruster area ratio, aerospike engine contour, and overall engine area ratio that maximizes or minimizes a multidisciplinary objective. Ideally, this objective would be based on a vehicle trajectory-sizing analysis. This vehicle sizing analysis would require an additional module for estimating the aerospike engine weight. For this sample problem, we will optimize a composite engine ISP ($Comp_{ISP}$) for RLV. Erikson

6

suggested using a composite index based on a weighting of 21% sea level and 79% vacuum performance.[17]

Aerospike Parameters

The cowl height and aerospike nozzle length are set to be 95% of the engine boundary dimensions given in Table 1. The aerospike nozzle sample geometry begins at the exit of the thruster (point A on Fig. 8). The slope of the first line segment (A to B) on the aerospike nozzle is set equal to the tangent of the thruster tilt angle (θ). A cubic polynomial is used to define the aerospike contour from point B to the end of the truncated section at point C. Because the cowl location, nozzle length, and base height are fixed for this sample problem, the aerospike contour is completely defined by the thruster area ratio, thruster angle, axial position of point B, and slope at point C. The thruster angle, the thruster area ratio, and the cowl location (point D) determine the coordinate of point A.
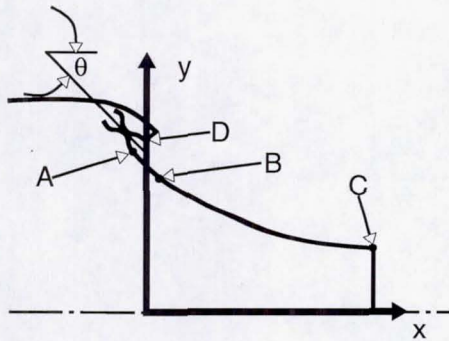

Fig. 8 Parametric aerospike nozzle surface.

The gas generator simulation is calibrated with the results of Erikson for a fuel inlet turbine temperature of 1900 °R.[17] In addition, we will assume that (1) all the losses total 5% of the ideal expansion, (2) 50% of the truncated spike thrust is recovered, (3) the base bleed mass flow needs to be 0.75% of the combustor flow, and (4) 75% of the freestream pressure is recovered on the base region when the exhaust wake is open. These numbers were selected for this sample problem and are not based on any specific design, analysis, or test data.

iSIGHT Framework Setup

To calculate the objective function required that the iSIGHT framework execute two different aerospike performance cases—one for sea level and one for near vacuum conditions. This was accomplished with the loop function in the iSIGHT framework and setting the altitude, mixture ratio, and power level based on the loop index. An initial optimization plan was specified was the gradient based procedure, Method of Feasible Directions. This method was selected from the iSIGHT framework's builtin suite of optimization methods.

iSIGHT Framework Results

The initial and final values of the design parameters are given in Table 2. A total of five design parameters were determined so that the sea level (SL) thrust for half of the engine would equal 260,000 lbf and the composite ISP was maximized. The sea level thrust constraint determines the maximum engine area ratio because the vehicle base dimension is fixed. The same design problem was solved twice with different initial values of the design parameters. The optimization algorithm quickly converged to a candidate solution for this initial set of variables.

Table 2: Method of Feasible Directions, Case 1 and 2

	Initial Value		Final Value	
Case	1	2	1	2
Parameters				
x_B (in.)	10	20	10.2	20.2
dy_C/dx	−0.20	−0.10	−0.187	−0.100
θ (°)	−45.0	−20.0	−34.4	−27.5
AR_{THR}	10	20	10.8	21.6
AR_{ENGINE}	193	193	199.	197.6
Constraint				
SL_{THRUST}(lbf)	264,018	251,531	260,000	260,001
Objective				
$Comp_{ISP}$ (s)	427.4	426.8	432.0	432.1

The final constraint and objective values obtained for the two cases are nearly identical, but the final design variables are significantly different. This could mean that either (1) there is a range of design parameters that yield similar results (robust design) or (2) that the gradient based method found a local minimum. To investigate the latter, a third case was solved by changing the optimization plan in the iSIGHT framework to use the genetic algorithm option.

Table 3: Genetic Algorithm, Case 3

	Lower Bounds	Upper Bounds	Final Results
Parameters			
x_B (in.)	9	45	43.9
dy_C/dx	−0.20	−0.075	−0.101
θ (°)	−45.0	−20.0	−28.2
AR_{THR}	5	25	19.3
AR_{ENGINE}	170	220	198.5
Constraint			
SL_{THRUST}(lbf)	—	—	260,000
Objective			
$Comp_{ISP}$ (s)	—	—	432.6

The results with the genetic algorithm option are shown in Table 3. The composite ISP objective was improved by 0.5 sec. when compared to the results of Case 2. While this improvement is significant, it is not enough of an improvement to make a change from the designs obtained in either Case 1 or 2 if they have some other advantage. This sample problem really shows that the aerospike engine design parameters picked have a fairly

large range of values that are near the maximum objective value.

This sample problem demonstrates how a multidisciplinary optimization tool can be used in a design process. The aerospike engine is significantly different than bell nozzle rocket engines, and additional benefits can be obtained by designing with a vehicle integration and performance approach. For a more practical design problem, we ultimately want to have the design based on a vehicle objective obtained from a trajectory analysis.

Summary

A methodology has been developed for use with the POST trajectory code in generating an aerospike engine database as a function of mixture ratio, power level, thrust vectoring, and altitude. The process for developing an aerospike engine database for conceptual vehicle design was presented. Typical characteristics of the aerospike engine performance versus altitude were discussed. This methodology was also imbedded into a multidisciplinary environment so that modified designs could be investigated. A sample design problem for modifying aerospike engine geometry was also presented.

References

[1]Sweetman, B., "VentureStar: 21st Century Space Shuttle," *Popular Science*, Oct. 1996, pp. 42–47.

[2]Baumgartner, R. I., and Elvin, J. D., "Lifting Body—An Innovative RLV Concept," AIAA Paper 95-3531, Sept. 1995.

[3]Rao, G. V. R., "Recent Developments in Rocket Nozzle Configurations," *ARS Journal*, Sept. 1961, pp. 1488–1494.

[4]Mueller, T. J., and Sule, W. P., "Basic Flow Characteristics of a Linear Aerospike Nozzle Segment," ASME Paper 72-WA/Aero-2, Nov. 1972.

[5]Rommel, T., Hagemann, G., Schley, C., Krülle, G., and Manski, D., "Plug Nozzle Flowfield Calculations for SSTO Applications," AIAA Paper 95-2784, July 1995.

[6]Hagemann, G., Schley, C. A., Odintsov, E., and Sobatchkine, A., "Nozzle Flowfield Analysis With Particular Regard to 3D-Plug-Cluster Configurations," AIAA Paper 96-2954, July 1996.

[7]Iacobellis, S. F., Larson, V. R., and Burry, R. V., "Liquid-Propellant Rocket Engines: Their Status and Future," *J. of Spacecraft and Rockets*, Vol. 4, Dec. 1967, pp. 1569–1580.

[8]Angelino, G., "On the Performance of Plug-Type Nozzles," *L'Aerotecnica*, Vol. 43, Jun. 1963, pp.101–110.

[9]Baftalovskii, S. V., Kraiko, A. N., and Tillyayeva, N. I., "Optimal Design of Self-Controlled Spike Nozzles and Their Thrust Determination at Start," AIAA Paper 99-4955, Nov. 1999.

[10]Morel, R., Dalbies, E., Le Fur, T., Schoeyer, H. F. R., Hufenbach, B., Immich, H., and Boman, A., "The Clustered Bell Aerospike Engine: Potential, Limitations and Preparation for Experimental Validation," IAF-95-S.2.04, Oct. 1995.

[11]Immich, H., and Caporicci, M., "FESTIP Technology Developments in Liquid Rocket Propulsion for Reusable Launch Vehicles," AIAA Paper 96-3113, July 1996.

[12]Tomita, T., Tamura, H., and Takahashi, M., "An Experimental Evaluation of Plug Nozzle Flow Field," AIAA Paper 96-2632, July 1996.

[13]Ito, T., Fujii, K., and Hayashi, A. K., "Computations of the Axisymmetric Plug Nozzle Flow Fields," AIAA Paper 99-3211, June 1999.

[14]Lockwood, M. K., "Overview of Conceptual Design of Early VentureStar Configurations," AIAA Paper 2000-1042, Jan. 2000.

[15]Brauer, G. L., Cornick, D. E., Habeger, A. R., Petersen, F. M., and Stevenson, R., "Program to Optimize Simulated Trajectories, Vol. 1," NASA CR-132689, April 1975.

[16]Schmucker, R. H., "A Simple Performance Calculation Method for LH2/LOX Engines With Different Power Cycles," NASA TM X-64749, Feb. 1973.

[17]Erikson, C., "Power Cycle Selection in Aerospace Engines for Single-Stage-to-Orbit (SSTO) Applications," AIAA Paper 97-3316, July 1997.

[18]Auslender, A. H., personal communication, NASA Langley Research Center, 1996.

[19]Korte, J. J., Salas, A. O., Dunn, H. J., Alexandrov, N. M., Follett, W. W., Orient, G. E., and Hadid, A. H., "Multidisciplinary Approach to Linear Aerospike Nozzle Optimization," AIAA Paper 97-3374, July 1997.

[20]Powell, W. B, "Simplified Procedures for Correlation of Experimentally Measured and Predicted Thrust Chamber Performance," NASA-CR-131519, April 1, 1973.

[21]*iSIGHT Designer's Guide*, Version 4.0, Engineous Software, Inc., Morrisville, NC, 1999.

[22]Follett, W. W., Ketchum, A. C., and Hsu, Y. F., "Optimization Methodology for Design of Three-Dimensional Rocket Nozzles," *ASME Proceedings FED-232*, Nov. 1995, pg. 87.

[23]Greer, H., "Rapid Method for Plug Nozzle Design," *ARS Journal*, April 1961, pp. 560–561.

[24]Angelino, G., "Approximate Method for Plug Nozzle Design," *AIAA Journal,* Vol. 2, No. 10, 1964, pp. 1834–1835.

[25]Rao, G. V. R., "Spike Nozzle Contour for Optimum Thrust," *Ballistic Missile and Space Technology*, edited by C. W. Morrow, Vol. 2, Pergamon Press, New York, 1961, pp. 92–101.

[26]Lee, C. C., and Thompson, D. D., "Computation of Plug Nozzle Contours by the Rao Optimum Thrust Method," NASA TM X-53078, 1964.

[27]Humphreys, R. P., Thompson, H. D., and Hoffmann, J. D., "Design of Maximum Thrust Plug Nozzles for Fixed Inlet Geometry," *AIAA Journal*, Vol. 9, Aug. 1971, pp. 1581–1587.

[28]Korte, J. J., "An Explicit Upwind Algorithm for Solving the Parabolized Navier-Stokes Equations," NASA TP-3050, Feb. 1991.

[29]Padula, S. L., Korte, J. J., Dunn, H., J., and Salas, A. O., "Multidisciplinary Optimization Branch Experience Using iSIGHT Software," NASA TM-1999-209714, Nov. 1999.